Fibrinogen−Catecholamine Interaction as Observed by NMR and Fourier Transform Infrared Spectroscopy

Silvia Martini, Marco Consumi, Claudia Bonechi, Claudio Rossi, and Agnese Magnani*

Department of Chemical & Biosystem Sciences, University of Siena, Via Aldo Moro, 2 − 53100 Siena, Italy, and Polo Universitario Colle di Val d'Elsa, Viale G. Matteotti, 15/16 − 53034 Colle di Val d'Elsa, (SI), Italy

Received March 7, 2007; Revised Manuscript Received May 11, 2007

In this work, the interactions between the main catecholamines—epinephrine and norepinephrine—and fibrinogen were investigated by NMR and Fourier transform infrared spectroscopies. The two hormones were found to interact with fibrinogen and to affect the protein secondary structure to a different extent. In particular, the protein selectively binds epinephrine at both the basal and stress concentrations, while it shows a weak nonspecific interaction with norepinephrine. The interaction with the stress level of epinephrine leads to drastic protein conformational changes, whereas norepinephrine does not affect fibrinogen secondary structure, even at stress concentration.

Introduction

Fibrinogen (Fbg) is a glycoprotein (MW = 341 kD) involved in the last step of the blood coagulation cascade by conversion to fibrin due to the proteolitic action of the enzyme thrombin. The Fbg molecule is formed by three couples of peptide chains, called Aα, Bβ, and γ.[1] Thrombin breaks four peptidic Arg−Gly bonds in the central region of the molecule, releasing two fibrinopeptides from the Aα and Bβ N-terminal chains. The monomeric fibrin with a $(\alpha\beta\gamma)_2$ structure spontaneously polymerizes to form a three-dimensional lattice.[2] This last step, in which the clot is formed, is characterized by the formation of Lys−Glu transversal bonds between monomers of fibrin and is catalyzed by the fXIIIa plasmatic factor activated by thrombin.

Fbg represents an essential factor in platelet aggregation.[3] Its main role in platelet adhesion involves the secondary formation of aggregates linked to the damaged vessel surface and the increase in the adhesion toward the majority of surfaces due to a preferential adsorption.[4−7] Blood Fbg level (200−250 mg/dl)[8] may change in pathological conditions. It increases in the presence of inflammations and decreases as a result of hyperfibrinogenlysis or disseminated intravascular coagulation. This process is induced by agonists such as thrombin and catecholamines.[9] The main catecholamines are epinephrine and norepinephrine. The release of catecholamines is regulated via the nervous system, and it is caused by physical, mental, and post-traumatic stress agents.[10] Epinephrine and norepinephrine act as neurotransmitters of the sympathetic nervous system on the adrenergic receptors, which mediate the cellular response to epinephrine and norepinephrine. They strongly stimulate α-adrenergic receptors, causing vessel constriction, β1-adrenergic receptors, increasing heart frequency, and α2 and β2-adrenergic receptors present at the articular and bronchial levels, whose procoagulant activity induces platelet activity.[11] Epinephrine, known as a powerful vessel constrictor and platelet activator, is more active than norepinephrine, as widely reported in the literature.[12−16] Previous studies have shown the differences regarding the plasma levels of the two hormones as well as their metabolic release mechanisms in response to different stresses.[17] However, the results strongly depend on the subject because of the tendency of norepinephrine concentration to slowly reach the basal level after the stimulus and are therefore difficult to generalize. Very high concentrations of epinephrine and norepinephrine (especially if they last in time) may cause an excessive platelet activation, resulting in thrombosis and coagulation defects.[18] Stress stimuli increase thrombin activity and fibrin turnover, in relation to β2-adrenergic receptors functioning and a concomitant catecholaminic reactivity.[11]

In this work, the interaction processes between Fbg and the two hormones have been investigated by NMR and Fourier transform infrared (FT-IR) spectroscopies with the aim to understand the role of epinephrine and norepinephrine in inducing protein conformational changes and, thus, their involvement in the platelet adhesion process.

Theory of NMR Analysis

In solution, the exchange of magnetic energy between excited nuclei and the lattice occurs mainly through dipole−dipole interactions between $I = 1/2$ nuclei. The efficiency of energy diffusion from "hot" nuclei (excited) to the "cold" lattice is a function of internuclear distances between nuclei and the modulation of these internuclear vectors by dynamical processes, typical of molecules in solution.

The time evolution of the *z*-component magnetization of two spins I and S in a dipolar interaction has the form[19,20]

$$\frac{d\langle I_Z\rangle}{dt} = -\rho_I(\langle I_Z\rangle - I_0) - \sigma_{IS}(\langle S_Z\rangle - S_0) \quad (1)$$

$$\frac{d\langle S_Z\rangle}{dt} = -\rho_S(\langle S_Z\rangle - S_0) - \sigma_{SI}(\langle I_Z\rangle - I_0) \quad (2)$$

where $\langle I_Z\rangle$ and $\langle S_Z\rangle$ and S_0 and I_0 are the *z*-components and the equilibrium values of magnetization of spins I and S, respectively, ρ_I and ρ_S are the direct self-relaxation rates, and $\sigma_{IS} = \sigma_{SI}$ are the "cross-relaxation" rates. In this case, the relaxation process assumes an exponential decay with a rate constant R_1, the spin−lattice relaxation rate:

* Corresponding author. Ph. +390577234385. Fax +390577234177. E-mail: magnani@unisi.it.

10.1021/bm070273n CCC: $37.00
Published on Web 08/18/2007

$$R_1^i = \rho_i + \sigma_{ij}\ (i = \mathrm{I, S}),\ (j = \mathrm{S, I}) \tag{3}$$

For multispin interaction, as occurs in complex systems of biomolecules, the "nonselective" spin−lattice relaxation rate R_1^{NS} of an i nucleus interacting with neighboring j nuclei can be described by a modified version of eq 3:

$$R_1^{NS} = \sum_{i \neq j} \rho_{ij} + \sum_{i \neq j} \sigma_{ij} \tag{4}$$

with the approximation of independent pairwise interactions.

The explicit forms of ρ_{ij} and σ_{ij} in the case of intramolecular dipolar interactions are

$$\rho_{ij} = \frac{1}{10} \frac{\gamma_H{}^4 \hbar^2}{r_{ij}{}^6} \left[\frac{3\tau_c}{1 + \omega_H{}^2 \tau_c{}^2} + \frac{6\tau_c}{1 + 4\omega_H{}^2 \tau_c{}^2} + \tau_c \right] \tag{5}$$

$$\sigma_{ij} = \frac{1}{10} \frac{\gamma_H{}^4 \hbar^2}{r_{ij}{}^6} \left[\frac{6\tau_c}{1 + 4\omega_H{}^2 \tau_c{}^2} - \tau_c \right] \tag{6}$$

where $\hbar$ is the reduced Plank's constant, γ_H and ω_H are the proton magnetogyric ratio and Larmor frequency, respectively, r_{ij} is the internuclear distance, and τ_c is the effective correlation time, which modulates the $i-j$ magnetic interaction.

When the excited i nucleus relaxes with j nuclei at their thermal equilibrium, the "cross-relaxation" term vanishes[21−23] (as the difference between the second terms of equations 1 and 2 becomes zero), and equation 4 becomes

$$Ri_1^{SE} = \sum_{i \neq j} \rho_{ij} \tag{7}$$

where R_{1i}^{SE} is the selective spin−lattice relaxation rate.

The explicit forms of the "nonselective" spin−lattice relaxation rate R_1^{NS} of an i nucleus interacting with neighboring j nuclei and the selective R_1^{SE} obtained by excitation of the i nucleus while the j nuclei are at thermal equilibrium are the following: [19,20−24]

$$R_1^{NS} = \frac{1}{10} \frac{\gamma_H{}^4 \hbar^2}{r_{ij}{}^6} \left[\frac{3\tau_c}{1 + \omega_H{}^2 \tau_c{}^2} + \frac{12\tau_c}{1 + 4\omega_H{}^2 \tau_c{}^2} \right] \tag{8}$$

$$R_1^{SE} = \frac{1}{10} \frac{\gamma_H{}^4 \hbar^2}{r_{ij}{}^6} \left[\frac{3\tau_c}{1 + \omega_H{}^2 \tau_c{}^2} + \frac{6\tau_c}{1 + 4\omega_H{}^2 \tau_c{}^2} + \tau_c \right] \tag{9}$$

The two spin−lattice relaxation rates—the selective R_1^{SE} and nonselective R_1^{NS}—which can be determined experimentally, show different dependence on molecular dynamics.[25]

In the fast motion regime typical of the free ligand ($\omega_0\tau_c \ll 1$), $R_1^{NS} > R_1^{SE}$, and in the slow motion regime, typical of a ligand bound to a macromolecule ($\omega_0\tau_c \gg 1$), $R_1^{SE} > R_1^{NS}$.

The spin−lattice relaxation rate of a ligand under conditions of fast chemical exchange between the free and bound states is described by

$$R_{1obs} = \chi_B R_{1B} + \chi_F R_{1F} \tag{10}$$

where R_{1obs} is the relaxation rate of the ligand in the presence of the macromolecule, R_{1B} and R_{1F} are the relaxation rates of the pure bound and free environments, respectively, and χ_B and χ_F are the molar fractions of the ligand in bound and free conditions, respectively.

If we consider the ligand−macromolecule equilibrium,

$$M + nL \leftrightarrows ML_n \tag{11}$$

with an equilibrium constant

$$K = \frac{[ML_n]}{[M][L]^n}$$

assuming $[L] \gg [M_0]$, it has been shown that

$$\Delta R_1 = \frac{K[L]^{n-1} R_{1B}}{1 + K[L]^n} [M_0] \tag{12}$$

where $\Delta R_1 = R_{1obs} - R_{1F}$, K is the thermodynamic equilibrium constant, and $[M_0]$ is the initial macromolecule concentration.

As suggested by eq 12, the plot ΔR_1 vs $[M_0]$ would have a straight line through the origin, with slope

$$[A]_L^T = \left(\frac{K[L]^{n-1} R_{1B}}{1 + K[L]^n} \right) \tag{13}$$

which is defined as the *affinity index* (l mol^{-1} s^{-1}).[26] The affinity index is a constant if temperature and ligand concentration are specified, as suggested by the T and L subscripts in the affinity index symbol.

The spin−lattice relaxation rate R_1^{SE} appears to be the best experimental parameter for obtaining information about ligand−macromolecule interactions. In conditions of fast chemical exchange between the free and bound environments, R_1^{SE} is expressed by the following equation:

$$R_{1obs}^{SE} = \chi_F R_{1F}^{SE} + \chi_B R_{1B}^{SE} \tag{14}$$

where R_{1obs}^{SE} is the experimentally determined selective relaxation rate, and R_{1F}^{SE} and χ_F and R_{1B}^{SE} and χ_B are the selective spin−lattice relaxation rates and the ligand fractions of the free and bound environments, respectively. Since $\chi_F + \chi_B = 1$, with reference to $\chi_B \ll 1$, eq 14 can be modified as

$$R_{1obs}^{SE} = R_{1F}^{SE} + \chi_B R_{1B}^{SE} \tag{15}$$

A significant contribution from the second term of eq 15 is possible only if $R_{1B}^{SE} \gg R_{1F}^{SE}$. These conditions apply when an interaction between the ligand and the macromolecule occurs.

A temperature dependency analysis of R_1^{SE} and R_1^{NS} is also required to test whether $R_1^{SE} > R_1^{NS}$ conditions are really due to a large $\chi_B R_{1B}$ term to R_1^{SE}; in fact, $R_1^{SE} > R_1^{NS}$ could also be the result of a reduction in molecular tumbling due to an increase in viscosity caused by the presence of a macromolecule in the solution. A reduction in both R_1^{SE} and R_1^{NS} with an increasing temperature demonstrates that the ligand fast motion condition $\omega_0\tau_c \ll 1$ holds in the solution. This allows the effects on R_1^{SE} to be attributed to the formation of the ligand−macromolecular complex.

In previous studies performed using this methodology, the affinity index was mainly calculated from selective relaxation rate enhancements calculated for a single proton, assuming an isotropic motion for the ligand molecule.[24,26,27] However, even for small ligands, there can be differences in the dynamics of different portions of the molecule, leading to effects on the selective relaxation rates and, as a consequence, on the affinity

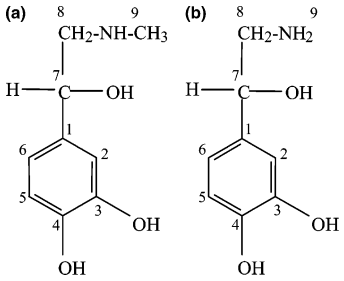

Figure 1. Structure and numbering of (a) epinephrine and (b) norepinephrine.

index value due to different correlation times modulating the dipolar interactions between protons at different positions. The normalization of $\Delta R_1^{SE} = R_{1obs}^{SE} - R_{1F}^{SE}$ to R_{1F}^{SE} removes the effects of different correlation times and different spin densities in the observed proton environment and isolates the effects of restricted motions due to the interaction of the ligand with the macromolecule.[28] The contribution of the bound ligand to the observed relaxation rate is now expressed as

$$\Delta R_{1N}^{SE} = \frac{KR_{1b}^{SE}[M_0]}{(1 + K[L])R_{1f}^{SE}} \tag{16}$$

The dependence of the normalized relaxation rate enhancements ΔR_{1N}^{SE} from the concentration of the macromolecule $[M_0]$ is represented by a straight line passing through the origin of the axes with slope

$$[A_I^N]_L^T = \frac{KR_{1b}^{SE}}{(1 + K[L])R_{1f}^{SE}} \tag{17}$$

$[A_I^N]_L^T$ is still a constant at fixed temperature and ligand concentration, and it is defined as the *normalized affinity index* ($dm^3\ mol^{-1}$).

Experimental

Materials. Epinephrine and norepinephrine (Figure 1a,b) were purchased from SIGMA and used without further purification. Fbg (Human Plasma, MW = 341 kDa) was purchased from CALBIOCHEM and used without further purification.

Methods. *NMR Measurements.* The solutions for the NMR experiments were obtained by dissolving the appropriate amounts of epinephrine and norepinephrine and Fbg in D_2O. ^1H NMR spectra were obtained on a Bruker DRX 600 spectrometer, operating at 600.13 MHz. The spin−lattice relaxation rates were measured using the $(180°\text{-}\tau\text{-}90°\text{-}t)_n$ sequence. The τ values used for the selective and nonselective experiments were 0.01, 0.02, 0.04, 0.06, 0.08, 0.1, 0.2, 0.4, 0.8, 1, 1.5, 2, 3, 4, 5, 7, and 20 s, respectively, and the delay time t in this case was 20 s. All the selective and nonselective spin−lattice relaxation rates refer to the H_6 proton of epinephrine and norepinephrine. The selective spin−lattice relaxation rates were calculated using the initial slope approximation and subsequent three-parameter exponential regression analysis of the longitudinal recovery curves. The maximum experimental error in the relaxation rate measurements was 5%. The affinity index was calculated by linear regression analysis of the experimental data.

IR Measurements. Solutions for the IR experiments were obtained by dissolving the appropriate amounts of ligand and protein in H_2O, in order to obtain the following concentrations: Fbg = 7.33×10^{-6} mol dm^{-3} (2 mg/mL); epinephrine = 50−60 pg/mL (basal concentration), 80−90 pg/mL (stress concentration); norepinephrine = 200−250 pg/mL (basal concentration), 400−500 pg/mL (stress concentration).

Instrumentation. The spectra were obtained with a Thermo FT-IR spectrometer Nicolet 5700, operating between 3000 and 900 cm^{-1}. An MCT detector was used, and the apparatus was purged with dry nitrogen. Typically, 300 scans at a resolution of 2.0 cm^{-1} were averaged. The frequency scale was internally calibrated with a reference He−Ne laser to an accuracy of 0.01 cm^{-1}. An attenuated total reflection (ATR) Barnes microcircle cell for liquid with germanium crystal was used to record the spectra in solution.

The collected IR spectra of Fbg−epinephrine and Fbg−norepinephrine do not contain the contribution of the two hormone vibrations, since the hormone concentrations used in the experiments were well below the IR detection limit. Because of its high surface activity, the Fbg, once the protein solution is introduced into the ATR cell, rapidly adsorbs onto the surface of Ge crystal. Since it is well-known that surface adsorption may affect the protein conformation,[29,30] spectra of both the protein and the protein−hormone systems were collected at predetermined intervals during their residence times (0−10 min) into the cell. The recorder spectra did not differ from each other, suggesting that the surface of the ATR Ge crystal did not significantly affect the Fbg secondary structure, at least within the experimental time interval (a few minutes).

Spectral Processing. All the spectra in solution were taken in a single beam mode. The sample spectrum was obtained by subtracting the solvent spectrum from the sample solution spectrum. The scale factor for solvent subtraction was chosen so that the spectral region between 2000 and 1700 cm^{-1} was flat.

Spectral Enhancement. In order to improve the observability of the overlapping bands, mathematical resolution enhancement was performed by a spectral deconvolution process that is similar to the Fourier self-deconvolution,[31,32] except that the mathematical operations are performed in the spectral domain rather than in the Fourier domain. The spectral deconvolution process moves intensity from the outer wings of a band to the center of the band, therefore reducing its effective half-width and improving its observability.[33] The quality of the deconvolution procedure is controlled by two variables, namely, a half-bandwidth of the Lorentzian line used for deconvolution and the resolution enhancement achieved.

Results and Discussion

NMR analysis. *Fbg−Epinephrine Interaction Analysis.* Figure 2a shows the ^1H spectrum of epinephrine with the resonance assignments. The signal chosen for the selective and nonselective measurements was the H_6 doublet at 6.77 ppm. Figure 2b reports the selective partially relaxed spectra of the adrenalin H_6 proton used to measure R_1^{SE}. Table 1 reports the experimental values of R_1^{SE} and R_1^{NS} in relation to Fbg concentration. Data show that, in the absence of the protein, the H_6 nonselective spin−lattice relaxation rate is bigger than the selective relaxation rate, while, increasing Fbg concentration, R_1^{SE} becomes greater than R_1^{NS}. This result suggests the existence of a strong contribution from the bound ligand fraction to the observed selective relaxation rate, supporting the hypothesis that interaction processes between epinephrine and Fbg occurred.

However, solutions containing relatively high concentrations of protein, as in this case, may be subject to an increase in viscosity, and this phenomenon may cause a slow down in the dynamics of the ligand, even in the absence of an interaction with the protein. If this occurs, the observed increase in the proton selective relaxation rate (i.e., the change from $\omega_0\tau_c \ll 1$ to $\omega_0\tau_c \gg 1$ motion conditions) may not be due to the formation of a ligand−receptor complex. The bell shape of R_1^{NS} versus $\omega_0\tau_c$ suggests that the effects of temperature changes on nonselective relaxation rates may be diagnostic, since an increase in temperature should cause a decrease in R_1^{NS} if the bulk

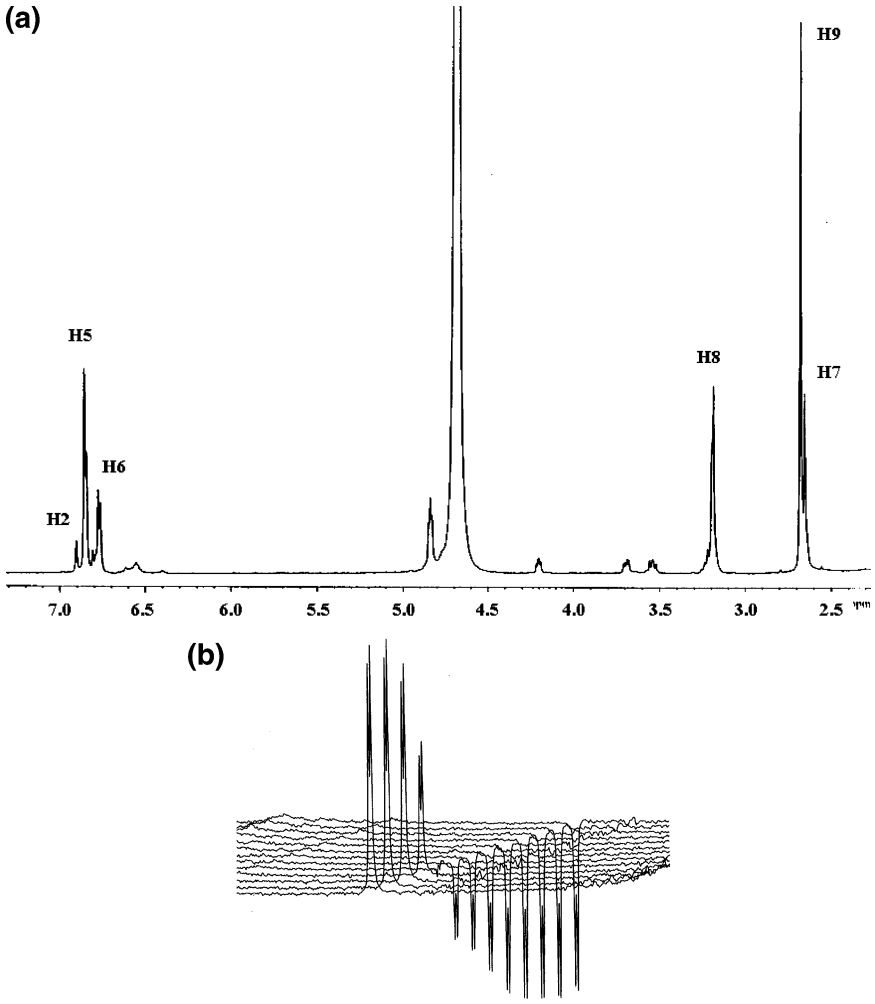

Figure 2. (a) Proton spectrum of epinephrine. (b) Selective partially relaxed aromatic proton spectra of a 2×10^{-2} mol dm^{-3} epinephrine solution. The selective measurements refer to the adrenalin H_6 proton recorded at 600 MHz.

Table 1. Experimental Values of Nonselective and Selective Spin−Lattice Relaxation Rates of the H_6 Proton of Epinephrine (2×10^{-2} M in D_2O) in the Presence of Variable Concentrations of Fbg (MW = 341K Da) at 298 K

Fbg concentration (mol dm−3)	R_1^{NS} (s^{-1})	R_1^{SE} (s^{-1})
0	0.81	0.77
1.46×10^{-6}	0.63	0.78
2.93×10^{-6}	0.60	0.83
5.86×10^{-6}	0.67	0.90
1.17×10^{-5}	0.66	1.01
2.34×10^{-5}	0.58	1.26
3.52×10^{-5}	0.67	1.53

Table 2. R_1^{NS} Values Calculated for the H_6 Proton of Epinephrine (2×10^{-2} mol dm^{-3}) in Relation to Temperature in the Presence of 12 mg/mL of Fbg

temperature (K)	R_1^{NS} (s^{-1})
300	0.61
308	0.53
316	0.44
323	0.31

ligand experiences fast motion conditions. In order to clarify this point for an epinephrine−Fbg system, a temperature-dependent analysis of the R_1^{NS} of the ligand in the presence of the macromolecule was performed. Table 2 reports R_1^{NS} values of the adrenalin H_6 proton in the presence of Fbg in relation to temperature. The observed decrease in R_1^{NS} with increasing temperature clearly indicates that the bulk ligand dynamics were not affected by the presence of the protein, that is, the free ligand experienced fast motion conditions even in the presence of Fbg.

In order to evaluate the strength of the interaction between Fbg and epinephrine, the *affinity index* was calculated from the slope of the straight line, obtained by linear regression analysis of selective relaxation rate enhancements, ΔR_1^{SE} ($\Delta R_1^{SE} = R_{1obs}^{SE} - R_{1F}^{SE}$), versus Fbg concentration. The affinity index for a Fbg−epinephrine system was found to be 21 500 mol^{-1} s^{-1} dm^3. As previously discussed in the theory section, motional anisotropies along the ligand molecule and different spin densities in the observed proton environment may affect the observed spin−lattice relaxation rates to some extent. In order to remove these effects,$[A]_L^T$ was normalized to the selective spin−lattice relaxation rate of the free ligand, and the *normalized affinity index* $[A^N]_L^T$ was calculated from the plot shown in Figure 3. $[A^N]_L^T$ was found to be 28 069 mol^{-1} s^{-1} dm^3.

Fbg−Norepinephrine Interaction Analysis. The NMR methodology used to investigate epinephrine−Fbg interactions was applied to study norepinephrine−Fbg systems. Table 3 reports R_1^{SE} and R_1^{NS} values calculated for the H_6 proton of norepinephrine in relation to Fbg concentration. The results show that both the nonselective and the selective relaxation rates of the H_6 proton of noradrenalin did not change appreciably with increasing Fbg concentration. This suggests a lack of specific

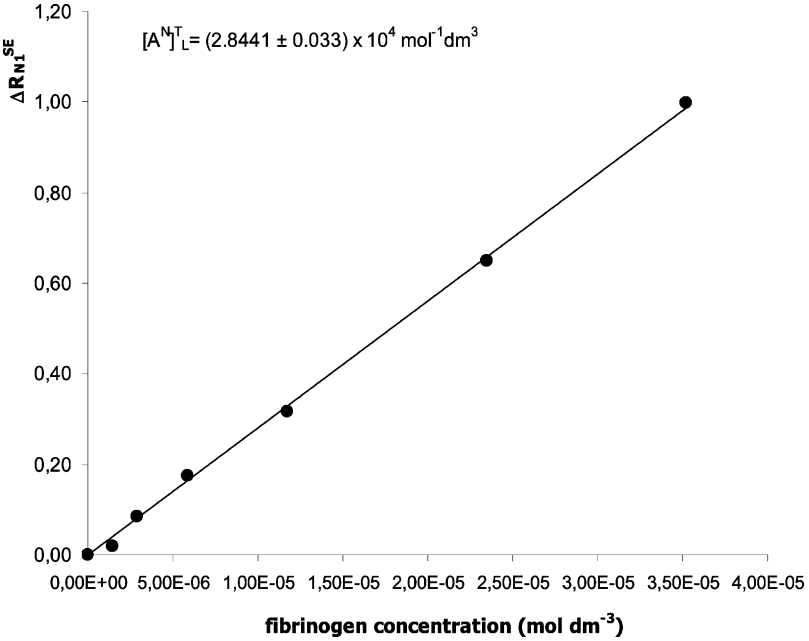

Figure 3. Linear regression analysis of epinephrine H_6 normalized selective relaxation enhancements, ΔR_{N1}^{SE}, as a function of Fbg concentration. The value of the normalized affinity index $[A_N]_L^T$ is also reported with the corresponding error. The measurements refer to a 2×10^{-2} mol dm^{-3} solution of epinephrine at 298 K.

Table 3. Experimental Values of Nonselective and Selective Spin−Lattice Relaxation Rates of the H_6 Proton of Norepinephrine (2×10^{-2} M in D_2O) in the Presence of Variable Concentrations of Fbg (MW = 341K Da) at 298 K

Fbg concentration (mol dm^{-3})	R_1^{NS} (s^{-1})	R_1^{SE} (s^{-1})
0	0.43	0.44
2.9×10^{-6}	0.49	0.44
1.17×10^{-5}	0.51	0.37
2.34×10^{-5}	0.53	0.41
2.93×10^{-5}	0.48	0.46

interaction processes between the ligand and the protein, in agreement with infrared analysis (see Infrared Analysis Section).

Infrared Analysis. Infrared spectroscopy was applied to the study of the two protein−hormone systems in order to identify the protein secondary structural changes induced by the hormone.

The structural changes were identified by the variations observed in the Amide I region of the protein infrared spectrum, which is assigned to the combination of the C═O stretching and N−H bending of the peptide group.[34] It is, in fact, well-known that the Amide I region is sensitive to changes in the protein secondary structure. The Amide I regions of the protein and protein−hormone systems were deconvoluted in order to better identify the vibrations associated with the single components of the protein secondary structure.

The original (spectrally subtracted) IR spectra of native Fbg in saline solution together with those of the two protein−hormone systems are reported in Figure 4. Figures 5 and 6 respectively show the deconvoluted spectra of the above-mentioned systems. Table 4 summarizes the main wavenumbers observed in the infrared spectra together with their assignments.

The IR spectra of the two protein−hormone systems (obtained as the difference between the spectrum of the protein−hormone system and that of the buffer) do not contain the contribution of the hormone vibrations. In fact, in both cases, the hormone concentrations used in the experiments were too low to allow the vibrational absorption of epinephrine and norepinephrine to be detected by IR. Thus, the wavenumbers observed in the spectra of the protein−hormone systems directly reflect the Fbg secondary structure in the presence of the hormones, and the variations observed in the spectrum of Fbg with respect to that of the native protein can only be assigned to the hormone-induced conformational changes of the protein.

This statement is also based on the fact that the effect of the ATR crystal surface on the protein conformation could be neglected. In fact, if significant protein conformational changes would be induced by the ATR crystal surface, they should be clearly observed in the spectra of both Fbg and Fbg−hormone systems. The Fbg secondary structure revealed by the spectra of Fbg and Fbg−norepinephrine instead corresponds to the conformation of the native protein,[35] whereas the spectra of Fbg−epinephrine reveal drastic conformational changes with respect to the native protein (especially when epinephrine reaches the stress level concentration). These findings strongly suggest the role of epinephrine in inducing significant conformational changes in Fbg, and, at the same time, they point out that the ATR crystal surface is not able to significantly affect the secondary structure of the protein within the time interval considered.

(a) Fbg−Epinephrine Systems. The comparison of the spectrum of a Fbg−epinephrine system with that of native Fbg (Figure 5) suggested the hypothesis of a protein−hormone interaction, indicating a protein conformational change induced by the hormone.

The presence of epinephrine, even at the basal (physiological: ≅60 pg/cm^3) level, in fact caused a drop in the Amide I band maximum. The Amide I band centered at 1650 cm^{-1} in the spectrum of native Fbg (spectrum a) shifted to 1630 cm^{-1} in the spectrum of the protein−epinephrine (spectrum b). This suggests an increase in the β-sheet component in the secondary structure of the protein accompanied by a decrease in its α-helix content.[36]

When the concentration of epinephrine in the Fbg solution was increased to the stress level (80−90 pg/mL), the changes in the protein infrared spectrum (spectrum c) increased as well, supporting the hypothesis of an interaction between Fbg and epinephrine that depends on hormone concentration. In spectrum

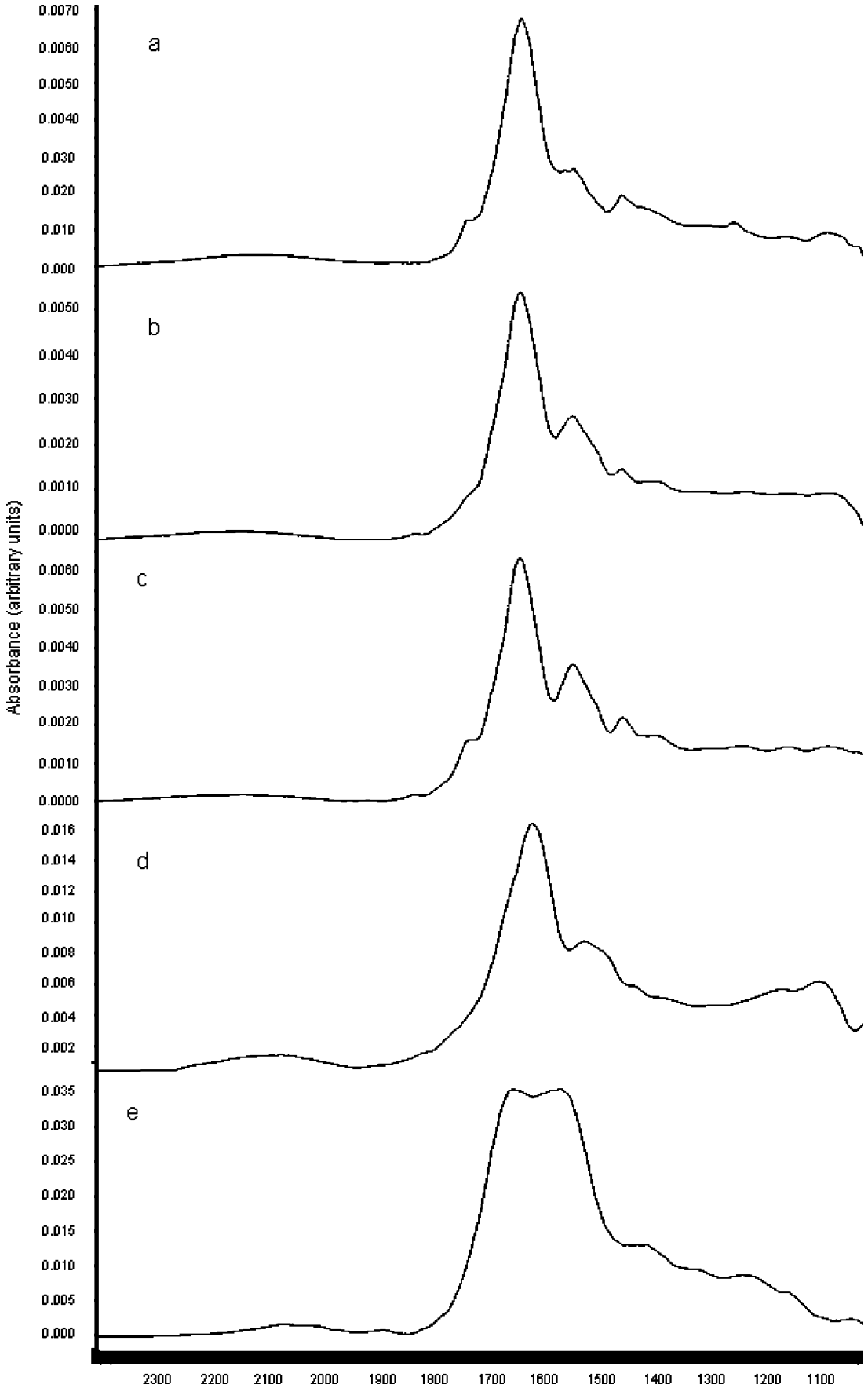

Figure 4. Difference infrared spectra of (a) native Fbg (2 mg/mL) in normal saline, (b) Fbg (2 mg/mL) and norepinephrine (200−250 pg/mL) in normal saline, (c) Fbg (2 mg/mL) and norepinephrine (400−500 pg/mL) in normal saline, (d) Fbg (2 mg/mL) and epinephrine (50−60 pg/mL) in normal saline, and (e) Fbg (2 mg/mL) and epinephrine (80−90 pg/mL) in normal saline.

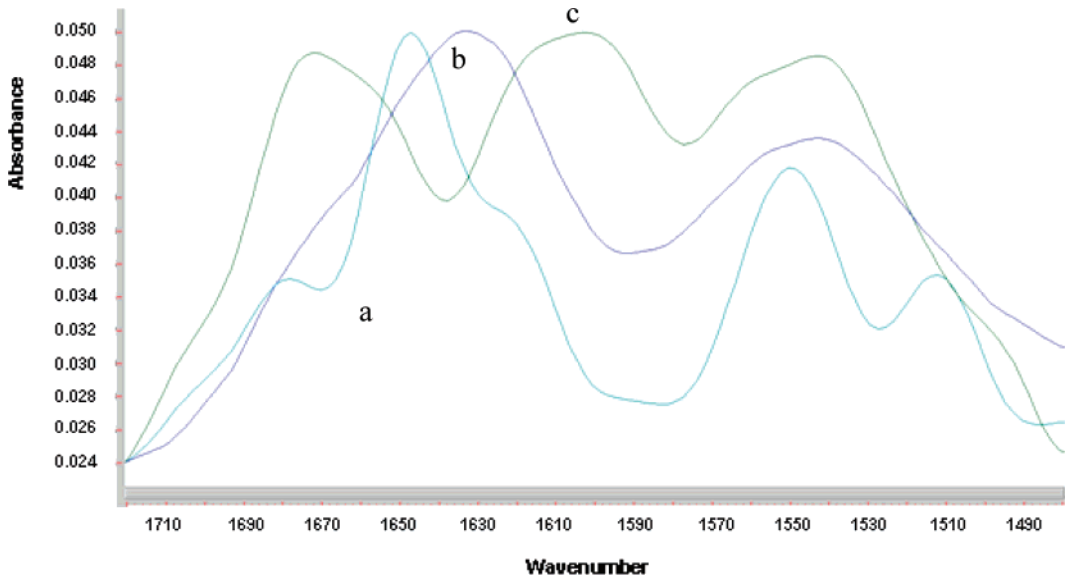

Figure 5. Deconvoluted infrared difference spectra of (a) native Fbg (2 mg/mL) in normal saline, (b) Fbg (2 mg/mL) and epinephrine (50−60 pg/mL) in normal saline, and (c) Fbg (2 mg/mL) and epinephrine (80−90 pg/mL) in normal saline.

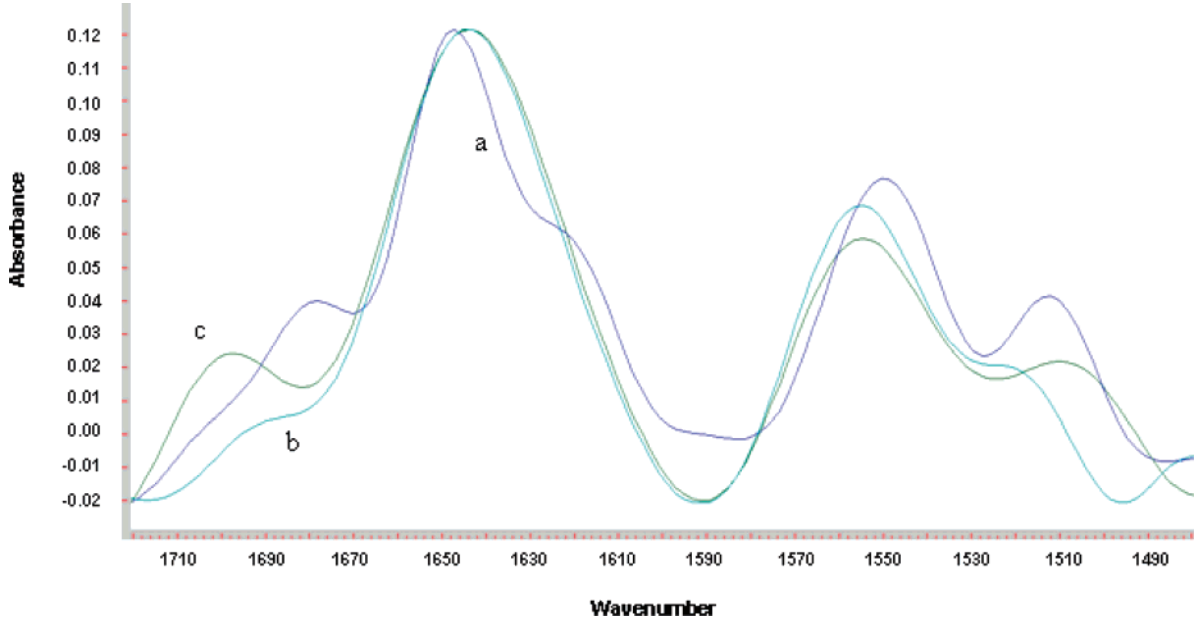

Figure 6. Deconvoluted infrared difference spectra of (a) native Fbg (2 mg/mL) in normal saline, (b) Fbg (2 mg/mL) and norepinephrine (200−250 pg/mL) in normal saline, and (c) Fbg (2 mg/mL) and norepinephrine (400−500 pg/mL) in normal saline.

Table 4. Main Wavenumbers Observed in the Fbg Amide I Spectral Range and Their Assignments in Terms of the Protein Secondary Structure

	Amide I band component (cm^{-1})[a]		
system	random-coil	α-**helix**	β-**sheet**
Fbg	1650 sh	1650 s	1625 sh
Fbg−epinephrine (basal concentration)	1670 sh	1635−1630 s	1620 sh
Fbg−epinephrine (stress concentration)	1675 s	1650 sh	1615−1600 s
Fbg−norepinephrine (basal concentration)	1690 sh	1645 s	1630 sh
Fbg−norepinephrine (stress concentration)	1695 sh	1645 s	1630 sh

[a] s = strong; sh = shoulder.

c, the intensity of the vibrational absorptions in the 1680−1660 cm^{-1} (random coil component) and 1630−1600 cm^{-1} (β-sheet and β-turn components) spectral ranges strongly increased with respect to the absorption at 1650 cm^{-1} (α-helix component), which showed the higher intensity in the spectrum of native Fbg.

In this case, the Fbg−epinephrine interaction led to a relevant increase in the random coil and β-sheet and β-turn components to the prejudice of the α-helix one, suggesting a radical conformational change in the protein.

(b) Fbg−Norepinephrine Systems. The infrared spectra of Fbg in the Fbg−norepinephrine systems did not differ as much as that of the native protein. The Amide I band remained centered at 1650 cm^{-1} even if the hormone concentration was increased to the stress level (400−500 pg/mL) (Figure 6). In this case, only an increase in the bandwidth was detected in the spectra of the Fbg−norepinephrine systems with respect to that of the native protein, suggesting the presence of a greater number of local protein microstructures, possibly due to the weak interaction with the hormone. However, the band shape did not change significantly neither in the case of hormone basal concentration

nor in the case of hormone stress level. Spectra b and c are almost superimposable, demonstrating that the increase in the hormone concentration in the protein solution is not reflected in a stronger protein conformational change. These findings suggest that the interaction between the two molecules, if any, is very weak and it does not depend on hormone concentration. Thus, the conformation of Fbg in solution in the presence of norepinephrine is substantially preserved.

The different behavior of the two hormones in affecting the Fbg conformation could be explained in terms of hormone molecular structure, even though epinephrine differs from norepinephrine only by the presence of a methyl group on the terminal amine moiety.

The NMR and IR data obtained for the protein−hormone systems clearly emphasized the basic role played by the ligand molecular structure in the "host−guest" molecular recognition process. Fbg selectively binds epinephrine as demonstrated by the high value of the affinity index determined by NMR measurements, and this specific protein−hormone interaction (which is ligand-concentration dependent) is reflected in the significant structural change of the protein, as proved by the drastic variation of the protein IR spectrum. Unlike epinephrine, norepinephrine is not selectively bound to Fbg, as pointed out by NMR measurements, although this molecule differs from epinephrine only for the lack of the CH_3 moiety. Moreover, the weak nonspecific interaction of norepinephrine with Fbg seems to be reversible, since it does not affect the protein conformation, as demonstrated by IR measurements.

Acknowledgment. The authors thank the Italian Interuniversities Consortium CSGI, MUR (PRIN 2005) and Fondazione Monte dei Paschi di Siena for financial support.

References and Notes

(1) Kieffer, N. In *The Role of Platelets in Blood−Biomaterial Interactions*; Missirlis, Y. S., Wautier, J.-L., Eds.; Kluwer Academic Publishers: Dordrecht, The Netherlands, 1993; pp 15−33.
(2) Hawiger, J. *Atheroscler. Rev.* **1990**, *21*, 165.
(3) Packham, M. A.; Evans, G.; Glynn, M. F.; Mustard, J. F. *J. Lab. Clin. Med.* **1969**, *73*, 686.
(4) Brash, J. L. In *Proteins at Interfaces: Physicochemical and Biochemical Studies*; Brash, J. L., Horbett, T. A., Eds.; ACS Symposium Series; American Chemical Society: Washington, DC, 1987; pp 490−506.
(5) Hawiger, J.; Timmons, S.; Kloczewiak, M.; Strong, D. D.; Doolittle, R. F. *Proc. Natl. Acad. Sci. U.S.A.* **1982**, *79*, 2068.
(6) Roushlati, E.; Pierschbacher, M. D. *Science* **1987**, *238*, 491.
(7) Pidard, D. *Pathol. Biol.* **1989**, *37*, 1107.
(8) Coller, B. S.; Peerschke, E. I.; Scuder, L. E.; Sullivan, C. A. *J. Clin. Invest.* **1983**, *72*, 325.
(9) Lam, N. Y.-L.; Rainer, T. H.; Ng, M. H.-L.; Leung, Y.; Cocks, R. A. *Resuscitation* **2002**, *55* (3), 277.
(10) Holmsen, H.; Weiss, H. J. *Annu. Rev. Med.* **1979**, *30*, 119.
(11) Ahlquist, R. P. *Am. J. Physiol.* **1948**, *153*, 596.
(12) Lefkowits, R. J.; Stadel, J. M.; Caron, M. G. *Annu. Rev. Biochem.* **1983**, *52*, 159.
(13) Lin, H.; Young, D. B. *Circulation* **1995**, *91*, 1135.
(14) Anfossi, G.; Trovati, M. *Eur. J. Clin. Invest.* **1996**, *26*, 353.
(15) Lanza, F.; Beretz, A.; Stierlè, A.; Hanau, D.; Kubina, M.; Cazenave, J. P. *Am. J. Physiol. (Heart Circ. Physiol.)* **1998**, *255* (24), H1276.
(16) Rao, G. H. R.; Escolar, G.; White, J. G. *Thromb. Res.* **1986**, *44*, 65.
(17) Bylund, D. B. *Pharmacol. Biochem. Behav.* **1985**, *22*, 835.
(18) Ruffolo, R. R.; Nicholas, A. J.; Stadel, J. M.; Hieble, J. P. *Pharmacol. Rev.* **1991**, *43*, 475.
(19) Bloch, F. *Phys. Rev.* **1957**, *105*, 1206.
(20) Solomon, I. *Phys. Rev.* **1955**, *99*, 559.
(21) Freeman, R.; Hill, H. D. W.; Tomlinson, B. L.; Hall, L. D. *J. Chem. Phys.* **1974**, *61*, 4466.
(22) Noggle, J. H.; Shirmer, R. E. *The Nuclear Overhauser Effect*; Academic: New York, 1971.
(23) Neuhaus, D.; Williamson, M. *The Nuclear Overhauser Effect in Structural and Conformational Analysis*; VCH Publisher: New York, 1989.
(24) Rossi, C.; Bastianoni, S.; Bonechi, C.; Corbini, G.; Corti, P.; Donati, A. *Chem. Phys. Lett.* **1999**, *310*, 495.
(25) Rossi, C. In *Encyclopedia of NMR*; Grant, D. M., Harris, R. K., Eds.; J. Wiley and Sons: New York, 1995; Vol. 7, p 4237.
(26) Rossi, C.; Donati, A.; Bonechi, C.; Corbini, G.; Rappuoli, R.; Dreassi, E.; Corti, P. *Chem. Phys. Lett.* **1997**, *264*, 205.
(27) Rossi, C.; Bonechi, C.; Martini, S.; Ricci, M.; Corbini, G.; Corti, P.; Donati, A. *Magn. Reson. Chem.* **2001**, *39*, 457.
(28) Martini, S.; Bonechi, C.; Casolaro, M.; Corbini, G.; Rossi, C. *Biochem. Pharmacol.* **2006**, *71*, 858.
(29) Lenk, T. J.; Ratner, B. D.; Gendreau, R. M.; Chittur, K. K. *J. Biomed. Mater. Res.* **1989**, *23*, 549.
(30) Barbucci, R.; Magnani, A. *Biomaterials* **1994**, *15* (12), 955.
(31) Blas, W. E.; Helsey, G. W. In *Deconvolution of Absorption Spectra*; Academic Press: New York, 1981.
(32) Kauppimen, J. K.; Moffat, D. J.; Mantsch, H. H.; Cameron, D. G. *Appl. Spectrosc.* **1981**, *35*, 271.
(33) *Instructions Infrared Data System* (CDS-3 Application Program Rev. D); Perkin-Elmer Corporation: Waltham, MA, 1985.
(34) Bellamy, L. J. *The Infrared Spectra of Complex Molecules*; Methuen: London, 1958.
(35) Gendreau, R. M. Biomedical fourier transform infrared spectroscopy: Application to proteins. In *Spectroscopy in the Biomedical Sciences*; Gendreau, R. M., Ed.; CRC Press: Boca Raton, FL, 1986; pp 21−52.
(36) Barbucci, R.; Lamponi, S.; Magnani, A. *Biomacromolecules* **2003**, *4*, 1506.

BM070273N